NASA CONTRACTOR REPORT

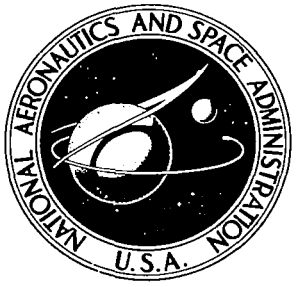

NASA CR-11

NASA CR-1149

THE EFFECTS OF A PLASMA IN THE NEAR-ZONE FIELD OF AN ANTENNA — II

by W. C. Taylor

Prepared by
STANFORD RESEARCH INSTITUTE
Menlo Park, Calif.
for Langley Research Center

NATIONAL AERONAUTICS AND SPACE ADMINISTRATION • WASHINGTON, D. C. • SEPTEMBER 1968

NASA CR-1149

THE EFFECTS OF A PLASMA IN THE NEAR-ZONE FIELD OF AN ANTENNA — II [Final report].

By W. C. Taylor

Prepared under Contract No. NAS 1-7024 by
STANFORD RESEARCH INSTITUTE
Menlo Park, Calif.

for Langley Research Center

NATIONAL AERONAUTICS AND SPACE ADMINISTRATION

For sale by the Clearinghouse for Federal Scientific and Technical Information
Springfield, Virginia 22151 – CFSTI price $3.00

ABSTRACT

A program of measurements is reported relating to the effects on an antenna caused by a plasma in the near field. In one phase of the program, admittance measurements were performed with a Teflon-plugged waveguide slot antenna radiating into the flowing ionized gas of an arc-driven shock tube. The electron density was varied above and below the critical density at two different values of shock-tube pressure. The results are compared with theoretical predictions.

In the other major portion of the program, measurements were made in the same shock tube to determine the ionization rise times in normal-shock-heated air and other planetary gas mixtures. The principal results of these measurements were to supply the ionization rise history in air and in a 90-percent N_2/10-percent CO_2 mixture over a wide range of pressures and shock speed.

CONTENTS

ILLUSTRATIONS

I INTRODUCTION

This is the Final Report on a one-year contract that is the third in a series. These three projects, each with a different emphasis, have dealt with the effects of a plasma in the near-zone field of an antenna. These studies have been generally aimed at the problem of communications during hypersonic flight through the atmosphere of the earth and other planets. The first of these was devoted to a study of small loops and dipoles in hydrocarbon-flame plasmas with relatively high collision frequency.[1]*

The emphasis of the second-year program[2] was on measurements with X-band radiating apertures with at least one dimension of the same order as the free-space wavelength. These measurements were made in both an RF plasma jet and a 12-inch, arc-driven shock tube. The operating regimes of pressure in both these facilities were such that the collision frequency was low compared with the RF. Included in the second-year program were a few admittance measurements of an open waveguide slot antenna in the plasma jet, and considerable reflection coefficient measurements of a similar slot in the shock tube.

In this third program, all the measurements were performed in the shock tube. Admittance measurements were performed on a waveguide slot antenna plugged with Teflon such that free-space mismatch was minimized. In addition, measurements of ionization rise times and electron densities were made in normal-shock-heated air and in mixtures of CO_2 and N_2. Knowledge of these parameters is important to both aerospace communication and to a better basic understanding of the transient phenomena occurring when gases are shock-heated. Concurrent theoretical programs in both the slot-admittance[3] and ionization rise-time[4] areas were performed at the NASA-Langley Research Center.

---

*References are listed at the end of this report.

This report includes in Sec. II a short description of the shock-tube facility, the primary measurements equipment, and the auxiliary apparatus. Section III is a summary of the slot-admittance measurement results, and Sec. IV gives results of the rise-time measurements.

The author is grateful to T. Morita, W. E. Scharfman, and J. B. Chown of SRI for many helpful discussions and suggestions. The measurements were capably performed by R. L. Warner, J. W. Granville, and C. D. Walker.

II DESCRIPTION OF FACILITIES AND MEASUREMENT PROCEDURES

A. Arc-Driven Shock Tube

The shock tube used in these studies is of the arc-driven type and is modeled after the design of Camm and Rose.[5] A schematic of the tube is presented in Fig. 1. Figure 2 shows a cross section of the shock-tube driver. A full description of performance capabilities is reported in Ref. 6. Near the end of this project, fabrication and installation of a new driver were completed. An alumina liner was used, rather than the Lexan, for purposes of reducing the impurities propelled into the test section from the driver. Whereas the Lexan ablated sufficiently during each firing to coat the inside walls of the tube with a carbonaceous layer, the alumina ablates much less per firing, giving both longer life and a much reduced wall impurity problem.[7]

The shock speed is measured by a series of flush probes mounted in the tube walls. The probe current develops a voltage across a resistor. This voltage is then differentiated to give a spike in voltage when the ionization front passes the probe. The voltage spike is applied to the vertical plates of a raster oscilloscope (see Fig. 3), and the time for the shock to travel a known distance is measured from the oscilloscope in terms of the time between spikes. The shock speed decreases as a function of distance from the driver; over the two-meter region of speed measurement, the deceleration is typically 5 to 10 percent.

B. Ion Probes

Ion probes were used in the shock tube for all measurements. For the admittance measurements, the probes were utilized to determine the absolute electron density as a function of time during a shot in a given location in the tube. For the rise-time measurements, it was necessary to determine only the relative ionization-density time history. Scharfman,[8,9] using microwave interferometers, demonstrated in earlier studies with air in the shock tube that 10-mil-diameter wire probes, biased for ion-saturation current, collect current density very nearly

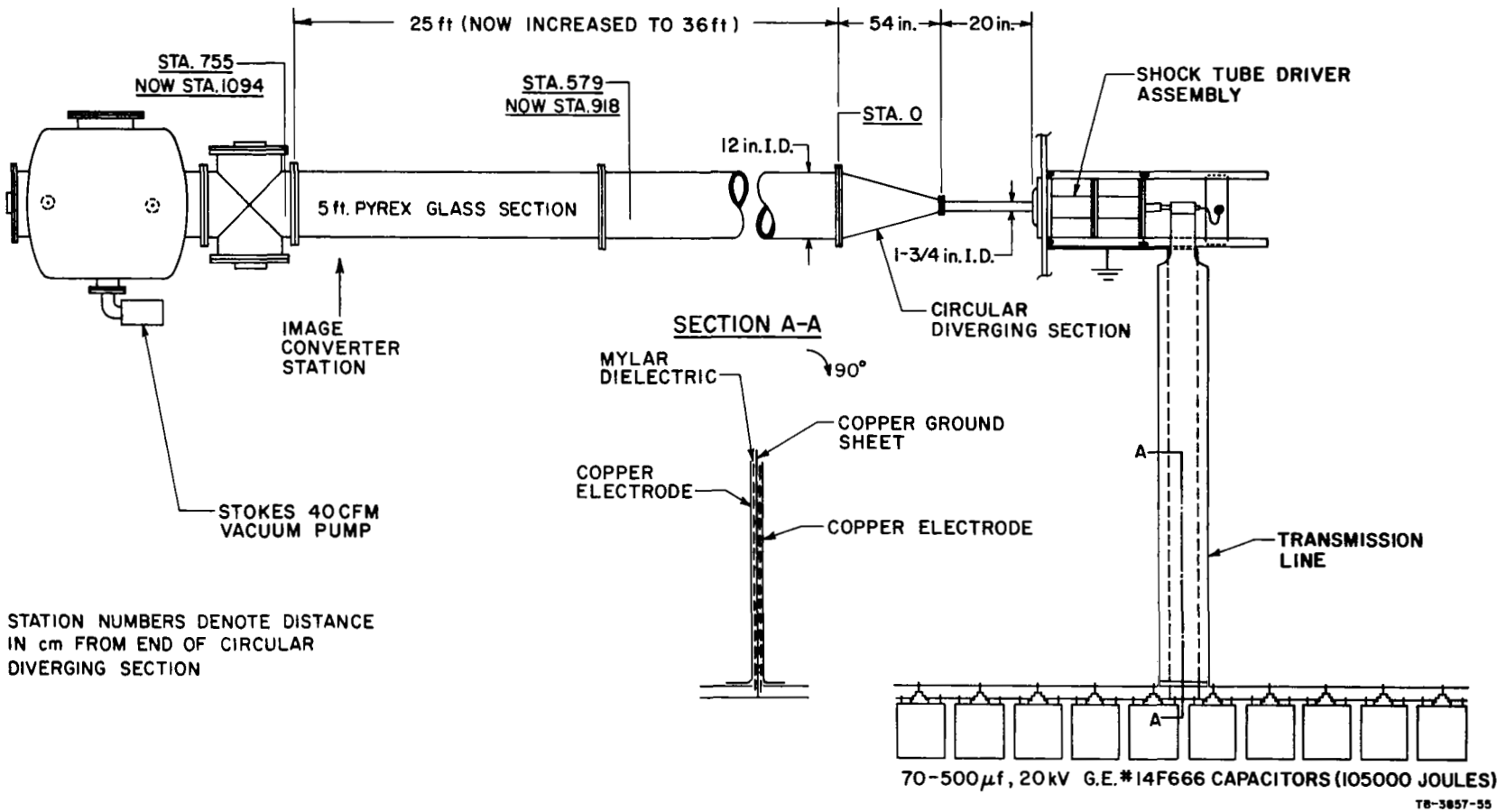

FIG. 1 SCHEMATIC LAYOUT OF ARC-DRIVEN SHOCK TUBE

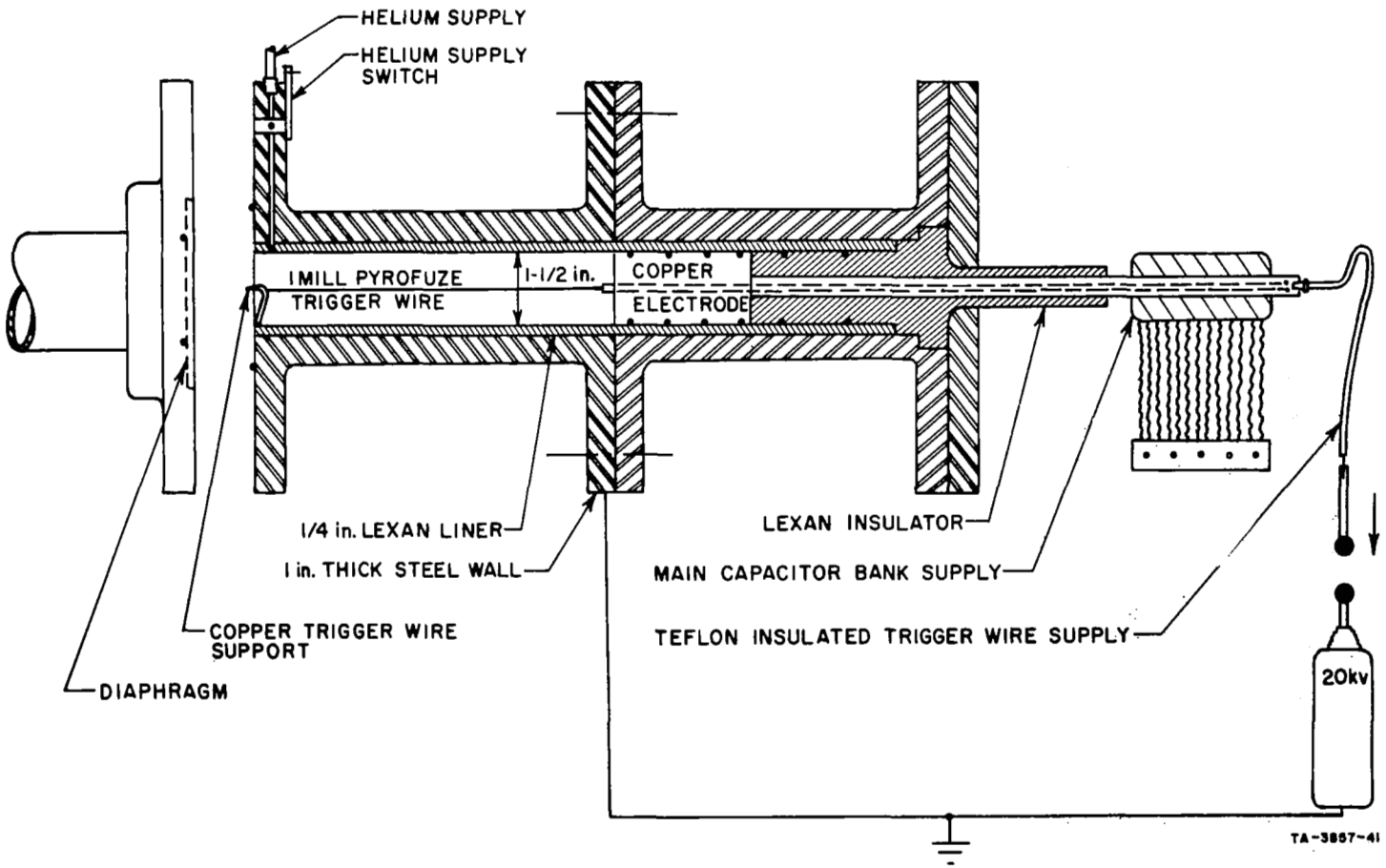

FIG. 2 CROSS SECTION OF SHOCK TUBE DRIVER

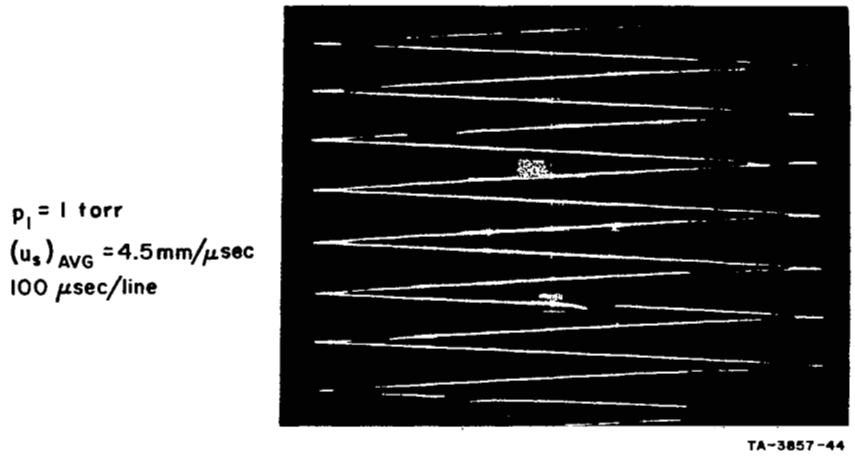

FIG. 3 SHOCK SPEED MEASUREMENT ON RASTER SCOPE

proportional to the free-stream ion density for initial shock-tube pressures, $p_1 \leq 0.1$ torr. The accuracy in inferring the density using existing theory over a wide range of electron density can be seen in Fig. 4, using simultaneous microwave interfereometer data as a standard. Figure 5 is a graph of the calculated proportionality "constant" for a 1/2-inch-long wire probe perpendicular to the flow.

For higher pressures, wedge-shaped probes of the type sketched in Fig. 6, with a 10-degree half-angle, were used. Scharfman[10] found that the oblique attached shock off such wedge probes in air produced additional ionization slowly enough so that the wedge probes also collect current density proportional to the free-stream ion density in the pertinent range of shock speeds for $p_1 \leq 1.0$ torr. The proportionality factor for the wedge probes can be deduced from theory approximately as well as for the wire probes and was essentially constant over the range of densities measured. Because of the proportionality demonstrated for both probes, the normal-shock ionization rise times were inferred directly from the saturation ion current record as a function of time. In some of the shots in air, simultaneous measurements of rise time inferred from the probe data and from microwave reflection data showed good agreement.

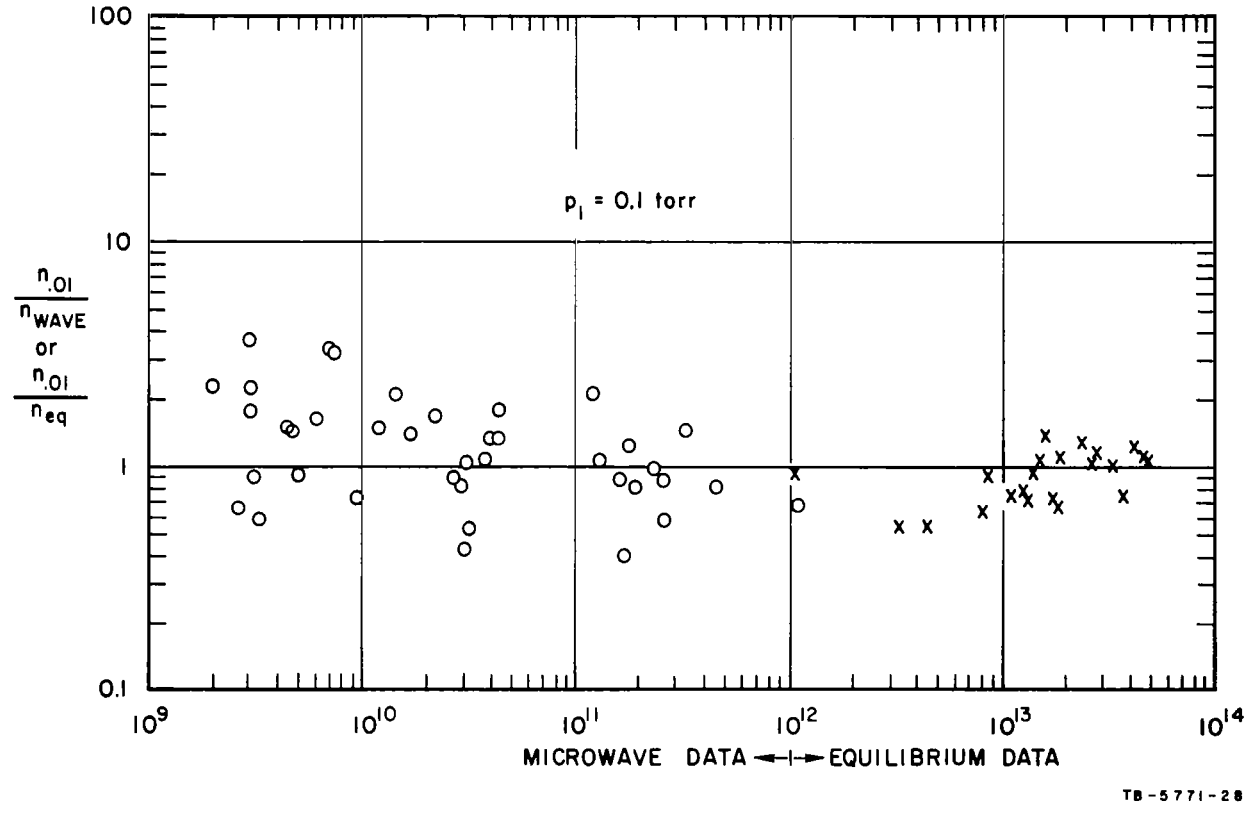

FIG. 4 RATIO OF ELECTRON DENSITIES INFERRED FROM 10-mil WIRE PROBES AND FROM MICROWAVE DATA AS A FUNCTION OF ELECTRON DENSITY INFERRED FROM MICROWAVE DATA

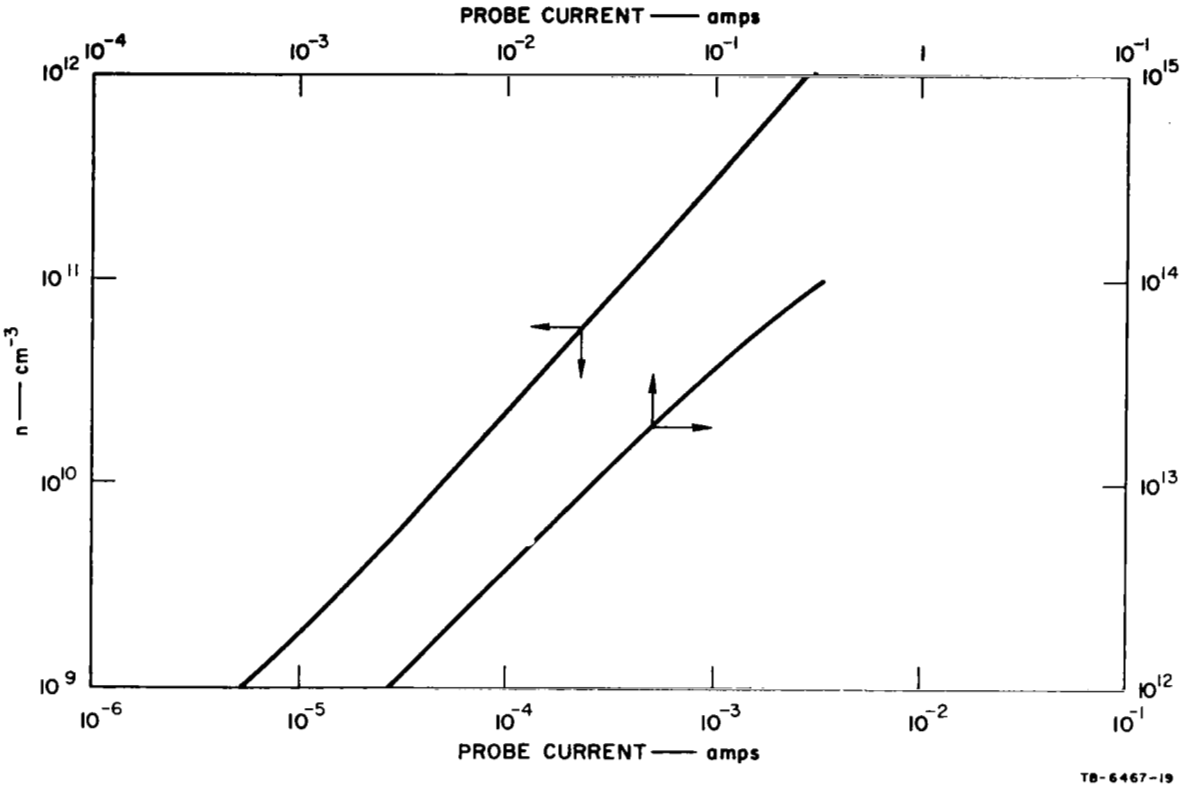

FIG. 5 THEORETICAL RELATIONSHIP BETWEEN PROBE CURRENT AND ION DENSITY FOR 10-mil BY ½-INCH WIRE PROBE PERPENDICULAR TO FLOW

It follows from the studies in air that the wedges are valid for making rise-time measurements over the same pressure/speed regimes in any gas with rise times no faster than air.

C. Antenna Admittance

The Teflon-plugged open-waveguide slot antenna is shown in Fig. 7. The leading edge of the slot ground plane was made sharp to minimize the effects on the flow, and the wedge-probe was used in the 1.0-torr shots to monitor the ion density just downstream of the aperture. In the 0.1-torr shots, a wire probe was placed in the same location. Prior studies[2] showed that a boundary layer of approximately 2-mm thickness would exist over the aperture in the 0.1-torr shots, compared with a 0.6-mm thickness in the 1.0-torr shots.

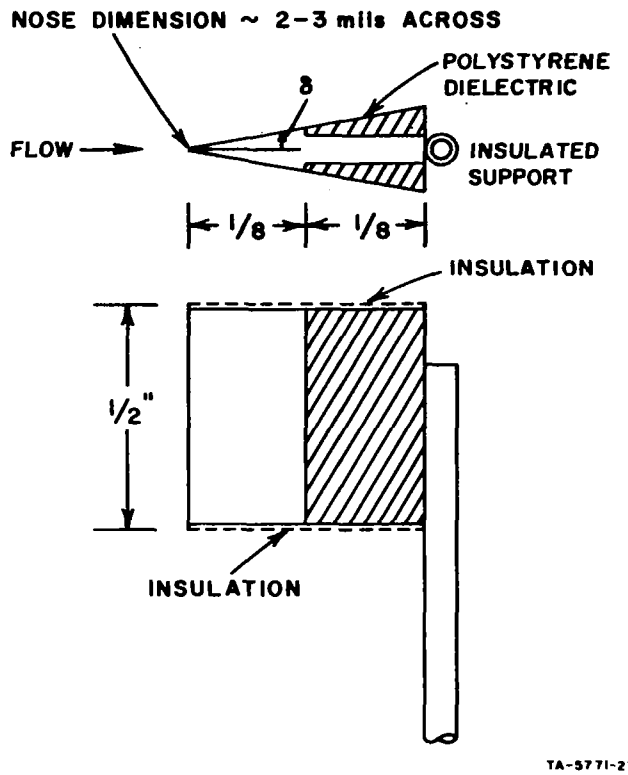

FIG. 6 SKETCH OF WEDGE PROBES

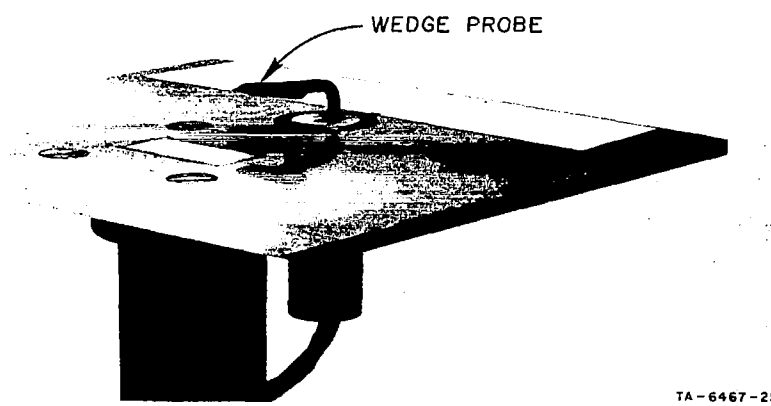

FIG. 7 PHOTOGRAPH OF TEFLON-PLUGGED WAVEGUIDE WITH GROUNDPLANE AND WEDGE PROBE IMMEDIATELY DOWNSTREAM OF SLOT

Because of the rapidly varying plasma conditions, the admittance measurements had to be made with fixed components using a CW microwave generator. It was decided to use a one-probe reflectometer similar to that described by Ginzton.[11] A block diagram of this apparatus is shown in Fig. 8. The detected signals from the reflected power and the slotted line probe were displayed along with the diagnostic probe currents as a function of time. During a shot, the slotted-line probe was fixed at a position either electrically identical to the aperture, or, for some shots, a quarter-wavelength from such a position. Construction of the simultaneous reflected and probe voltages in a vector diagram on a Smith chart directly determines normalized admittance.

The Teflon plug was cut to a length (0.41 inch) such as to cancel out the aperture free-space capacitive susceptance. The small remaining mismatch was due to the difference in conductance. Bends in the waveguide were avoided between the slotted line and the aperture to avoid introduction of spurious susceptance. Bench measurements were made primarily to compare the phase measurements of the one-probe technique with the slotted-line minimum/maximum technique using various terminations, including the free-space aperture. The average error in the reflection coefficient angle was 5 degrees. Significantly greater precision could have been achieved by using a second probe at a different electrical location in the slotted line, especially when the impedance of the aperture varied only slightly from the free-space admittance, as at low electron densities. However, increased precision in phase measurements was not deemed necessary as the emphasis of the program was shifted to the ionization rise-time measurements.

D. Mass Spectrometer

A quadrupole mass spectrometer was used to monitor the constituents of the gases into which the shocks were launched, largely to make a quantitative determination of the impurities present. A moderate flow of shock-tube test gas was bled off through a small valve in the tube wall. This gas was monitored then by bleeding off a much smaller flow of the gas into the ionizer and analyzer of the mass spectrometer.

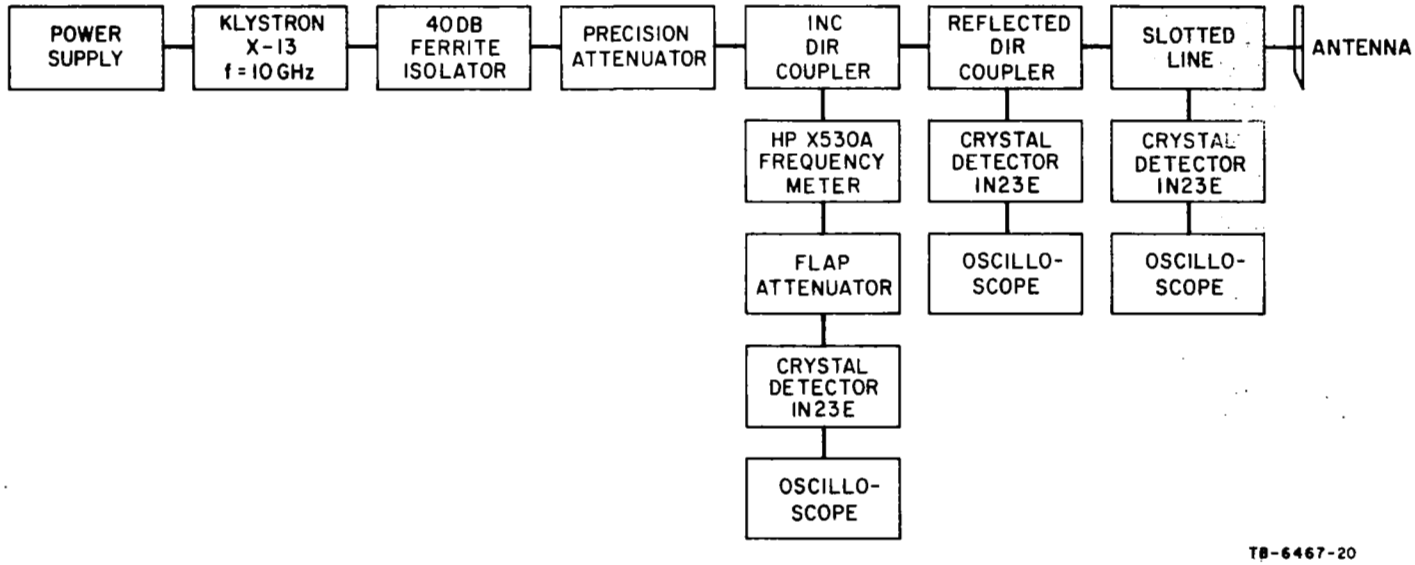

FIG. 8 BLOCK DIAGRAM OF ONE-PROBE REFLECTOMETER USED FOR ADMITTANCE MEASUREMENTS

Figure 9 is a photograph of the spectrometer and associated equipment connected to the shock tube in the background.

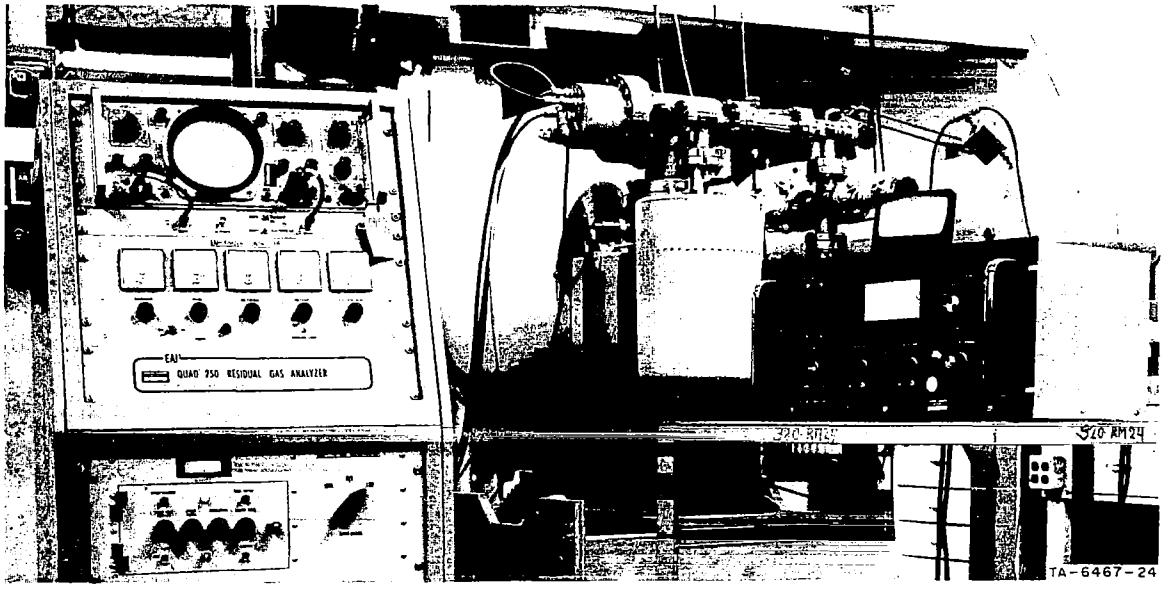

FIG. 9 PHOTOGRAPH OF MASS SPECTROMETER CONNECTED TO SHOCK TUBE

When a moderate-sized vacuum pump was used (throughout the first eight months) to keep the tube pumped down, it was found that water vapor, from the room air leaking into the tube, would accumulate up to 0.01-torr partial pressure or more when the tube was maintained at about 0.02-torr measured pressure. Thus, even when additional air was brought into the tube to raise the pressure to 0.1 torr for the low-pressure shots, water vapor constituted about 10 percent of the gas present. To reduce this impurity, a vessel for liquid nitrogen was installed inside the shock-tube dump tank. When the liquid nitrogen was introduced into the vessel, the water vapor would condense rapidly on the walls of it. The reduction in water-vapor content to about 1 percent by this method is illustrated by the two recorded mass spectra shown in Fig. 10. In Fig. 10, the peaks corresponding to helium and argon are inordinately high because the Vac-Ion pump in the residual gas analyzer (RGA) is inefficient in removing these gases.

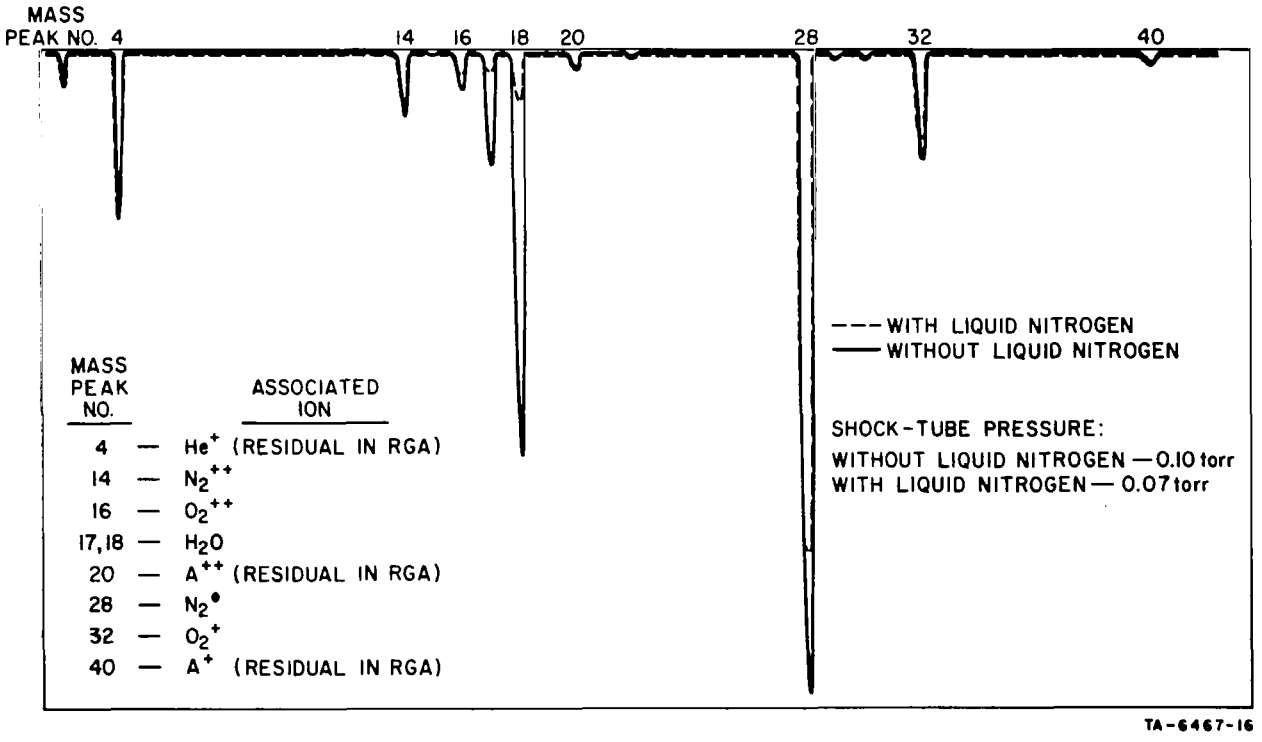

FIG. 10 MASS SPECTRA SHOWING EFFECTS OF LIQUID NITROGEN ON H_2O CONTENT IN SHOCK TUBE

The shock-tube wall impurities were analyzed, with the following results:

Element	Percent by Weight, Solid Impurity	Probable Source
C	35	Lexan Liner
Cu	18	Copper Electrode
Fe	15	Steel Diaphragm, Fuse Wire
Pd	4.2	Fuse Wire
Sn	3.6	Fuse Wire
Ni	3.0	Fuse Wire
Pb	3.0	Fuse Wire
Cr	3.0	Fuse Wire
Si	2.4	Fuse Wire

Many additional elements were found in concentrations less than 1 percent, probably the most important of which was sodium at approximately 0.05 percent. However, the mass spectrometric measurements of the shock-tube gases showed no sodium detectable in measurements capable of resolving approximately 50 parts per million.

III RESULTS OF ADMITTANCE MEASUREMENTS

A. 0.1-Torr Data

The admittance measurements were made at two different values of initial shock-tube pressure, p_1 = 0.1 torr and 1.0 torr, over a wide range of electron density values. It is estimated that in the 0.1-torr shots, the ratio of free-stream collision frequency ν to radian RF frequency ω was 0.06. The boundary layer thickness δ was estimated from previous measurements[1] to be 2.0-mm thick. For the 1.0-torr shots, $\nu/\omega \approx 0.4$ and $\delta \approx 0.6$ mm. Figure 11 shows an example of the time-varying output of the two microwave outputs and a wire ion probe just downstream of the aperture. On this 0.1-torr shot, the microwave probe was fixed at a point electrically equivalent to the aperture position in the transmission line.

It was found in earlier studies in 0.1-torr shots in air that the wire probes continue to diagnose the local plasma after the passage of the test slug (sometimes called HGS--homogeneous gas sample). However, on many shots, just following the slug, large oscillations in electron density are observed as the region of turbulent mixing of air and driver gases follows the slug over the aperture. Figure 12 illustrates this point, showing the measured admittance points plotted on a Smith chart, compared with predictions by Swift.[3] The ratio of the electron density n to critical density n_c is shown for both theoretical and experimental points. The circular data points for Fig. 12 as well as for most of Fig. 11 were taken from regions of slow electron density changes. It is seen that good agreement for these points is obtained in impedance, and the corresponding electron densities agree within a factor of two. However, when points are taken from the shots data at random, including the rapidly changing regions, greater scatter is apparent in the data. This increased scatter is probably caused by transverse nonuniformity in the plasma over the aperture as indicated by rapid variations observed by the sensors. Values of n/n_c are not available for some of the higher-susceptance points because the probe-current traces went off-scale for

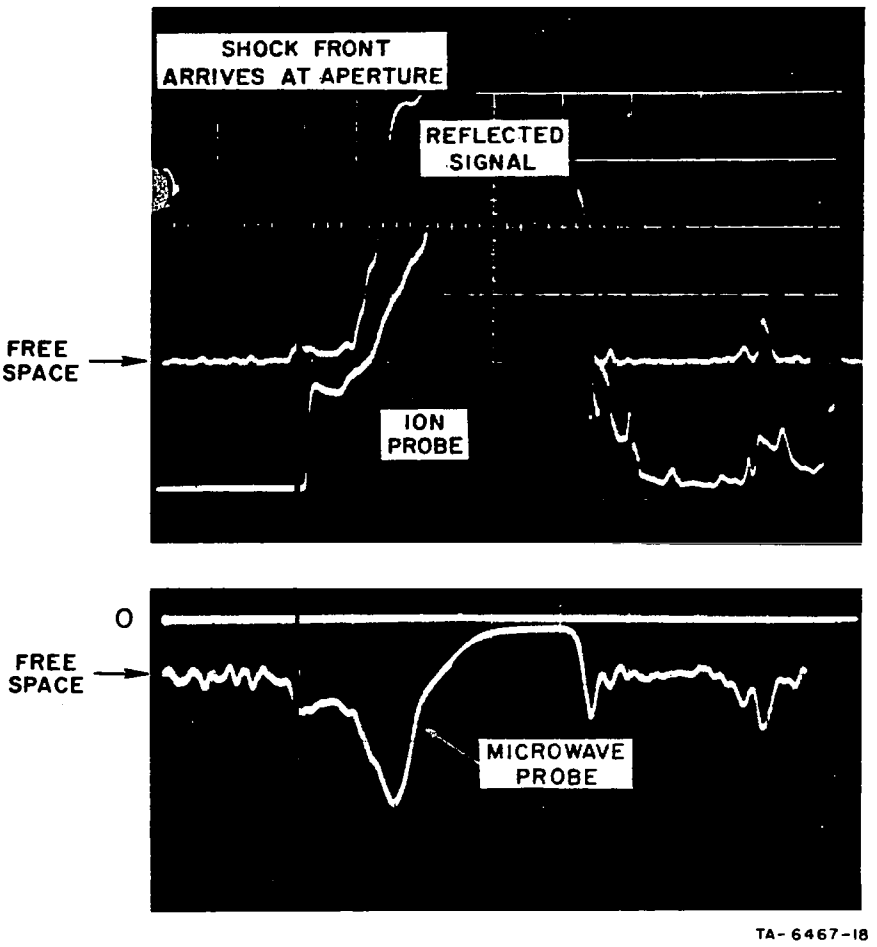

FIG. 11 SIMULTANEOUS OUTPUTS OF REFLECTED SIGNAL, ION PROBE, AND MICROWAVE PROBE DURING 0.1-TORR SHOT

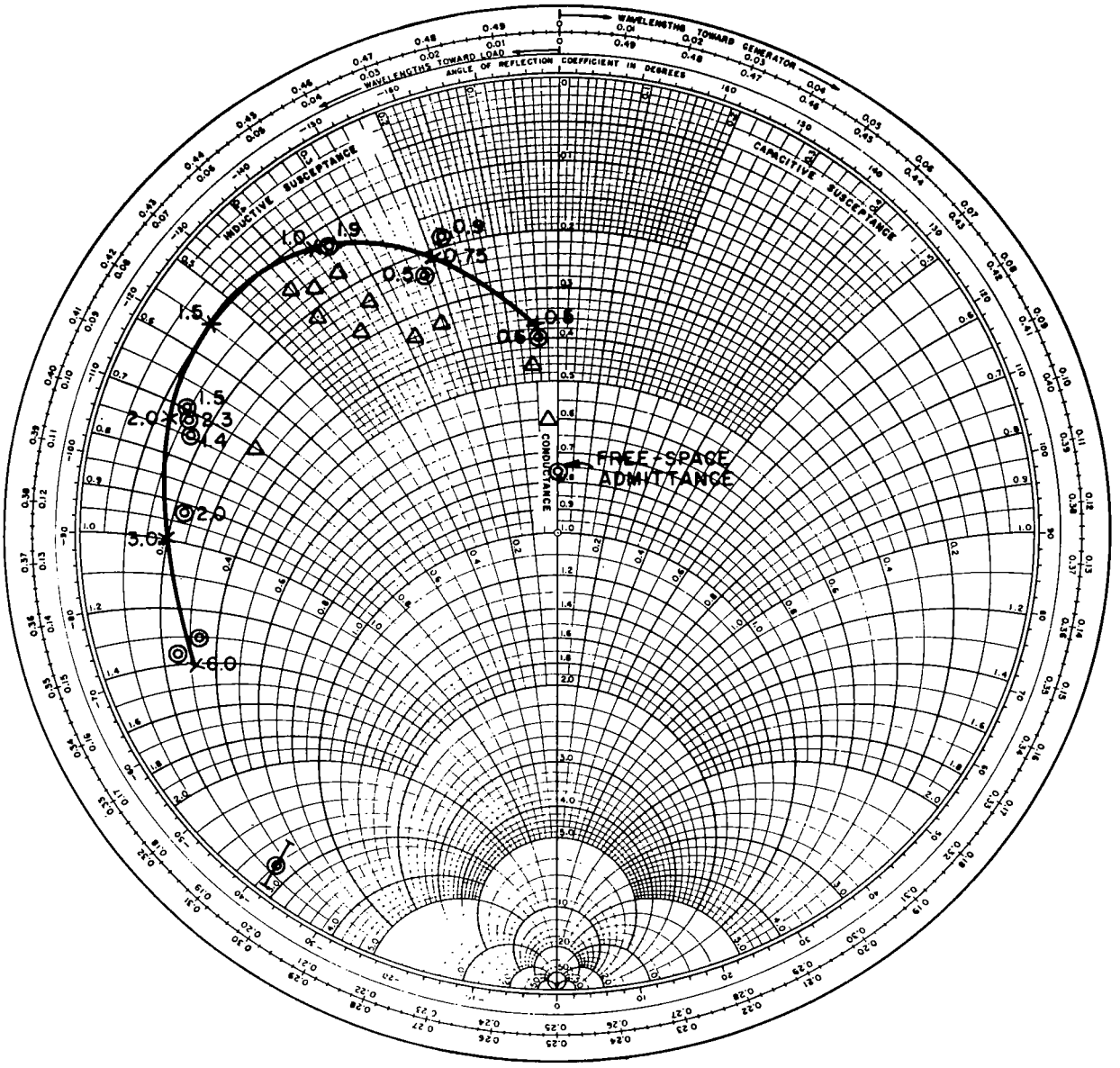

◎ DATA FROM SLOWLY VARYING PLASMA

△ DATA FROM RAPIDLY VARYING PLASMA

-×-×- THEORETICAL PREDICTIONS FOR 2mm BOUNDARY LAYER

NUMBERS DENOTE n/n_c RATIO FOR ADJACENT POINT

TA-6467-22

FIG. 12 SMITH CHART PLOT OF 0.1-TORR ADMITTANCE DATA COMPARED WITH THEORY

these points. The highest-susceptance data point in Fig. 12 was estimated from the point in Fig. 11, where the microwave probe signal reached the broad minimum about 70 μs after the front arrived.

In Fig. 13 the conductance and susceptance values of Fig. 12 are plotted separately against $n/n_c = (\omega_p/\omega)^2$.

B. 1.0-Torr Data

The admittance results from the higher-pressure shots are similar to the low-pressure ones in that good agreement with predictions is obtained when the plasma is slowly varying. Figure 14 illustrates this point similarly to Fig. 12. Figure 15 shows the admittance data of Fig. 14 broken down into susceptance and conductance, plotted against $(\omega_p/\omega)^2$.

C. Discussion

It is noted in Figs. 12 and 13 that almost all the data show a systematically higher conductance than predicted. The near agreement of the susceptance data with theory suggests that δ is no greater than 2 mm. Reference 12 contains a discussion of the dependence of conductance upon rather minute details of the boundary-layer electron density profile, especially for low ν/ω. Since this profile was not measured in this program of measurements, it is expected that much of the lack of agreement is due to inaccuracies in the profile estimates used in the calculations.

The data shown in Fig. 15 indicate that the assumed value of $\delta = 0.6$ mm is reasonable for the 1.0-torr shots, but a systematic error (in the other direction) is evident in the conductance again. Here, again, profiles were deduced from earlier work and at a different pressure, such that inaccurate profiles may be the overriding cause of the disagreement.

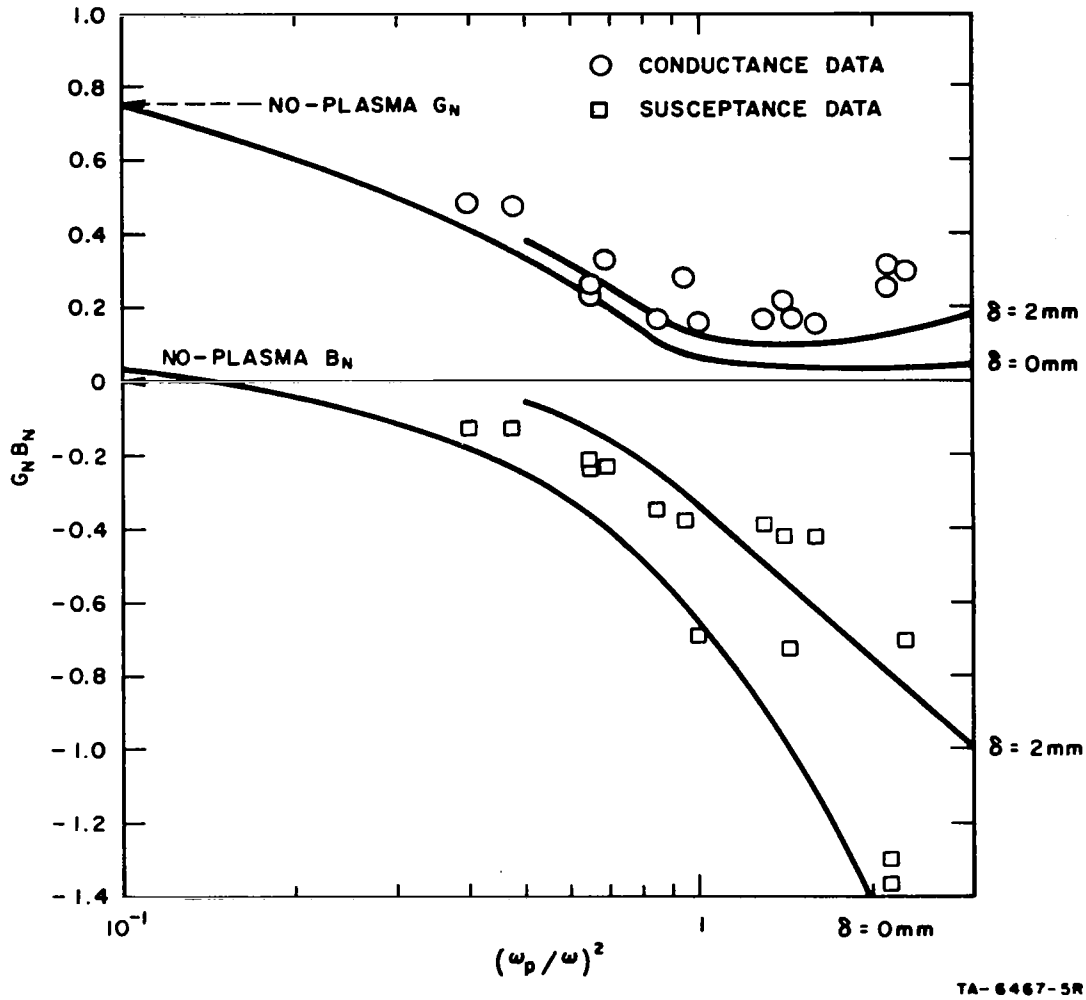

FIG. 13 MEASURED ADMITTANCE DATA, TEFLON-PLUGGED SLOT (0.1 torr) COMPARED WITH THEORY

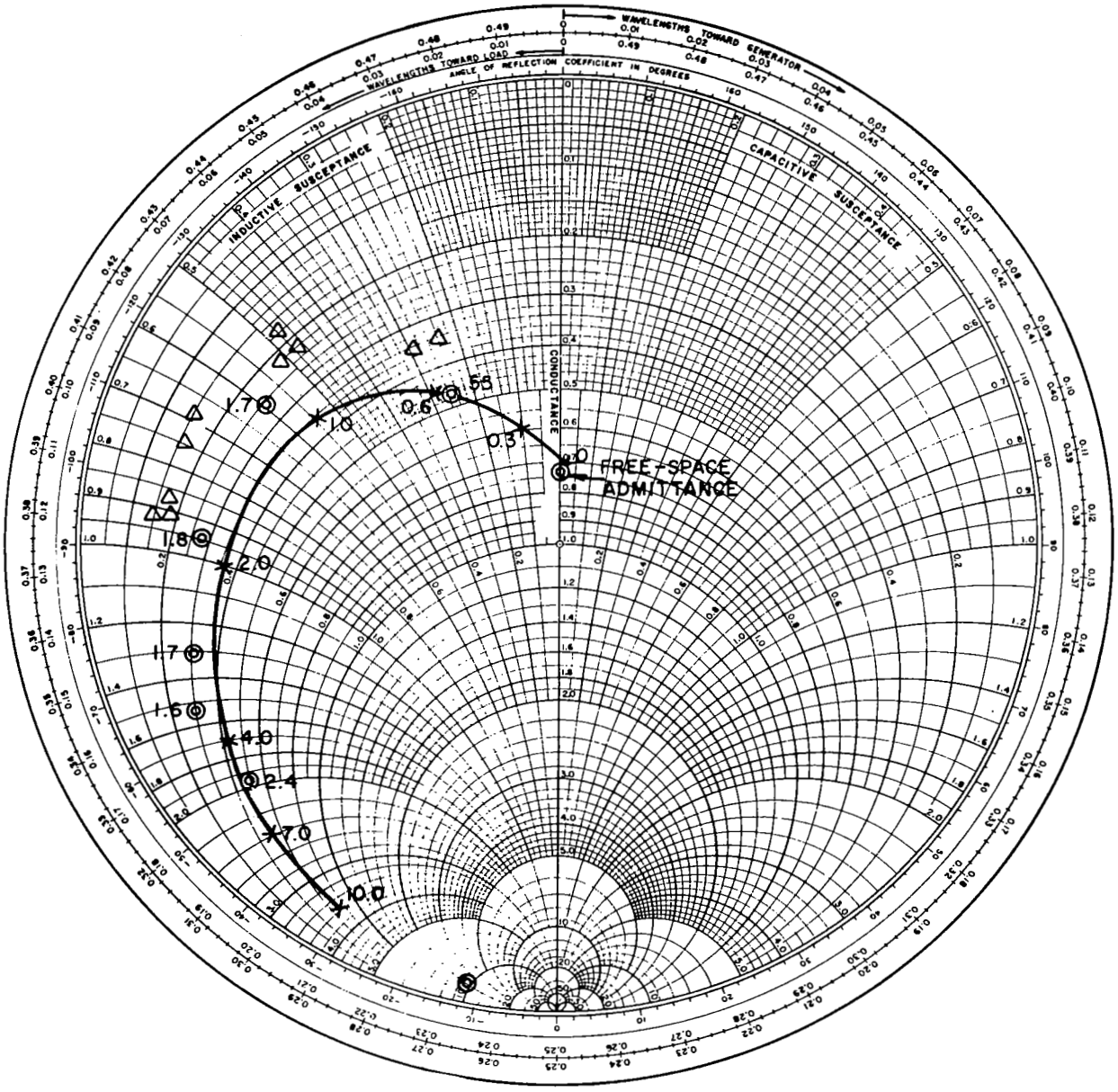

◎ DATA FROM SLOWLY VARYING PLASMA

△ DATA FROM RAPIDLY VARYING PLASMA

-✕✕- THEORETICAL PREDICTIONS FOR 0.6mm BOUNDARY LAYER

NUMBERS DENOTE n/n_c RATIO FOR ADJACENT POINT

TA-6467-21

FIG. 14 SMITH CHART PLOT OF 1.0-TORR ADMITTANCE DATA COMPARED WITH THEORY

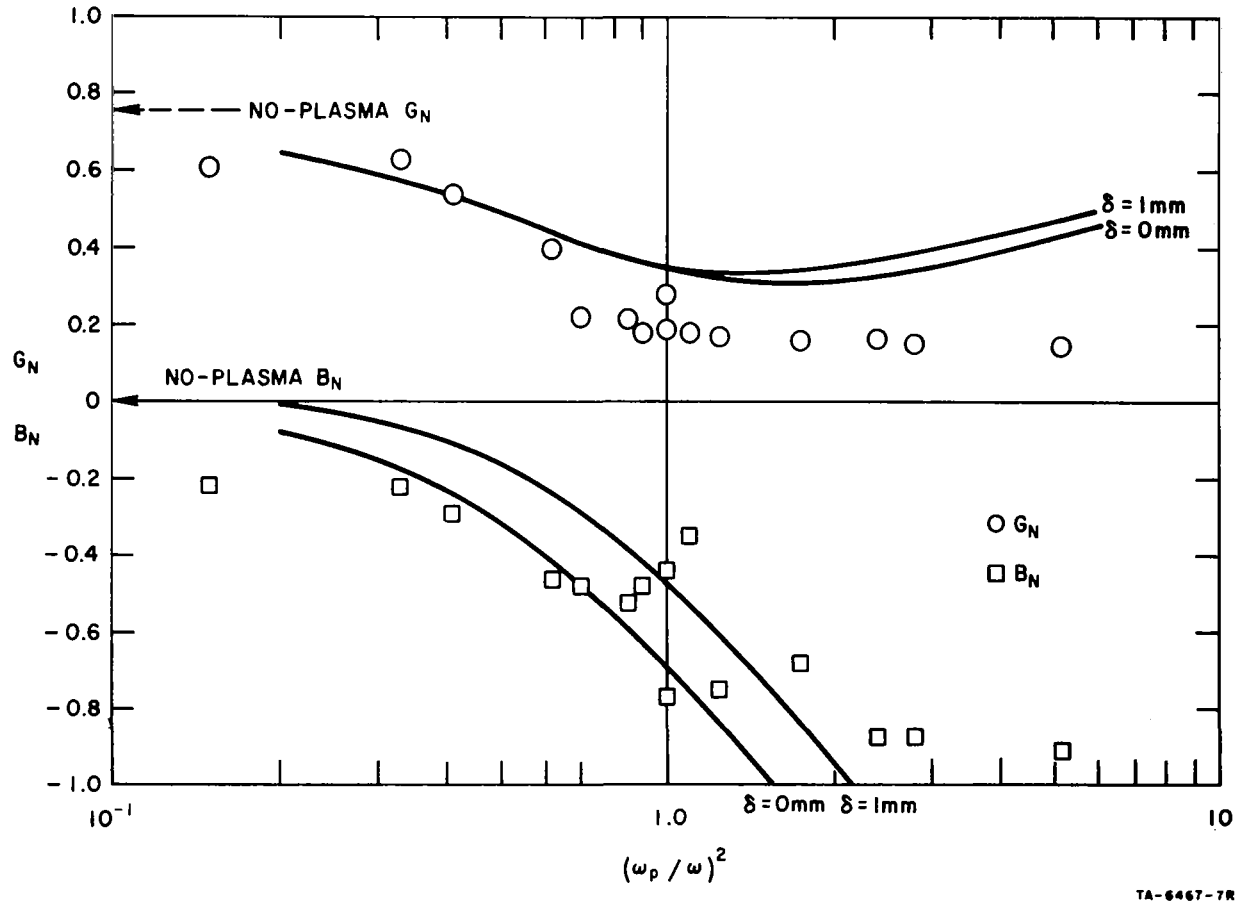

FIG. 15 MEASURED ADMITTANCE DATA, TEFLON-PLUGGED SLOT (1.0 torr), COMPARED WITH THEORY

IV RESULTS OF RISE-TIME MEASUREMENTS

A. Air

Figure 16 shows a plot of measured values of $p_1\tau$ in air as a function of shock Mach number, where p_1 is the initial shock-tube pressure, $\tau = n_{eq}/(dn/dt)_{max}$, and n_{eq} is the equilibrium value of electron density.* The solid curve represents the calculations of Thompson,[13] using adjusted rate constants to fit the earlier data of Frohn and deBoer[14] at the low-speed end and the data of Lin, Neal, and Fyfe[15] at the high-speed end. It is seen that the new data, taken at various values of p_1, covers nearly three orders of magnitude of the product $p_1\tau$ in a range where no data existed.

Figure 17 is an example of oscillograms of the ion current as a function of time, collected in these tests. The low-level initial rise shown in both traces is a current transient, seen at these and lower electron density levels, that is related to the approach of the ionized front through the dc electrostatic fields between the probes and the (grounded) tube walls.

Figure 18 shows a summary of results of measurements of n_{eq} for several different conditions. In "dry air" (H_2O no greater than 1 percent), the measured values agreed with theory within the capability of the ion probe measurement. However, it is apparent that 10 percent or more of water vapor caused a significant decrease in n_{eq}.

DeBoer[16] earlier reported rise-time measurements much faster than those of Frohn and deBoer,[14] but he cautioned that these early results should be considered as tentative because of shock-tube impurities. However, considerably less care was taken to eliminate impurities in the

---

*The nominal shock-tube test time is usually not long enough to observe n_{eq} if n overshoots. For these cases, the definition of measured τ is $n_{peak}/(dn/dt)_{max}$.

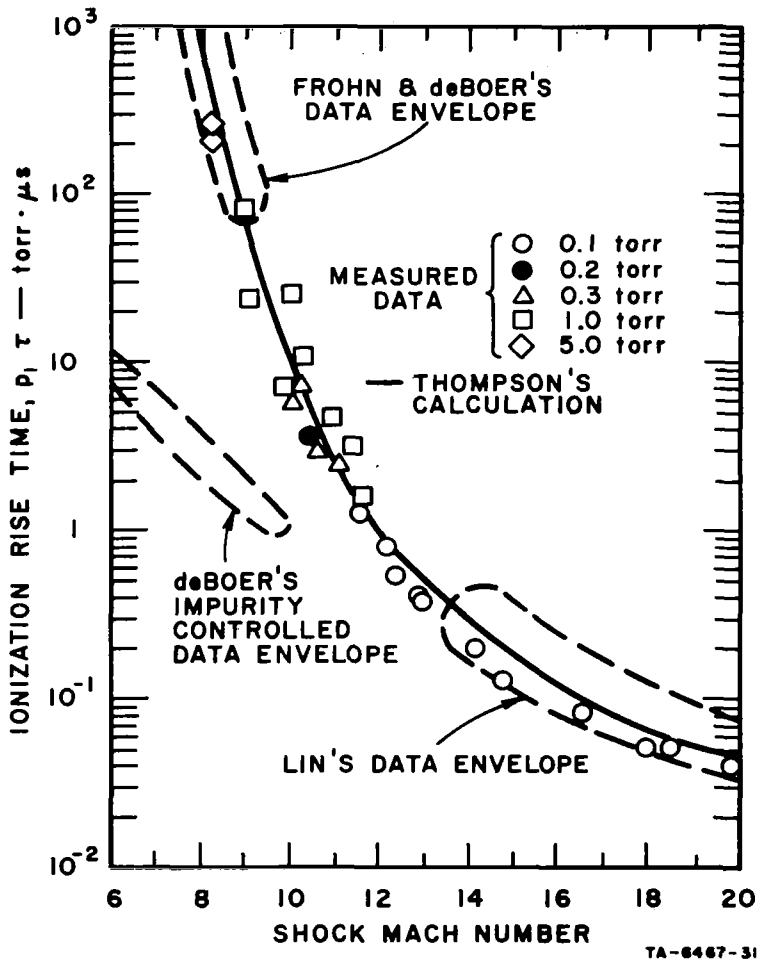

FIG. 16 MEASURED IONIZATION RISE TIMES IN AIR AS A FUNCTION OF SHOCK MACH NUMBER COMPARED WITH PREVIOUS WORK

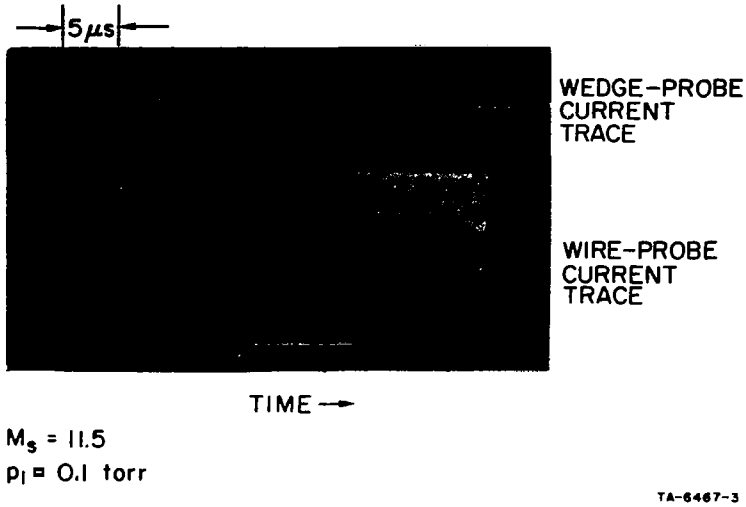

FIG. 17 ILLUSTRATION OF RISE-TIME MEASUREMENT USING TWO DIFFERENT ELECTROSTATIC PROBES

measurements reported here than in the work of Frohn and deBoer, and yet there is a good mating of the two sets of data. In one series, the driver-generated impurities were allowed to collect on the tube walls for approximately 60 shots without cleaning, yet neither this nor the 10-percent water vapor affected the air rise-time results. Tests with the new alumina liner give data quite similar to earlier results for a given shock speed.

The limit in measuring long rise times in our tube results because of the problem in distinguishing the legitimate transient rise in ionization level from the rise in level due to shock deceleration, monitored as the slug passed the ion probe. For example, a gas sample, shocked 2 meters upstream of a probe, passes the probe 40 to 60 μs after the front. If the front decelerates 7 percent during that 2-meter length, the n_{eq} associated with the gas sample is a factor of about five higher than that associated with the local shock speed. Unless the gradient just behind the front is considerably steeper than that, it is impossible to determine where the initial transient ends.

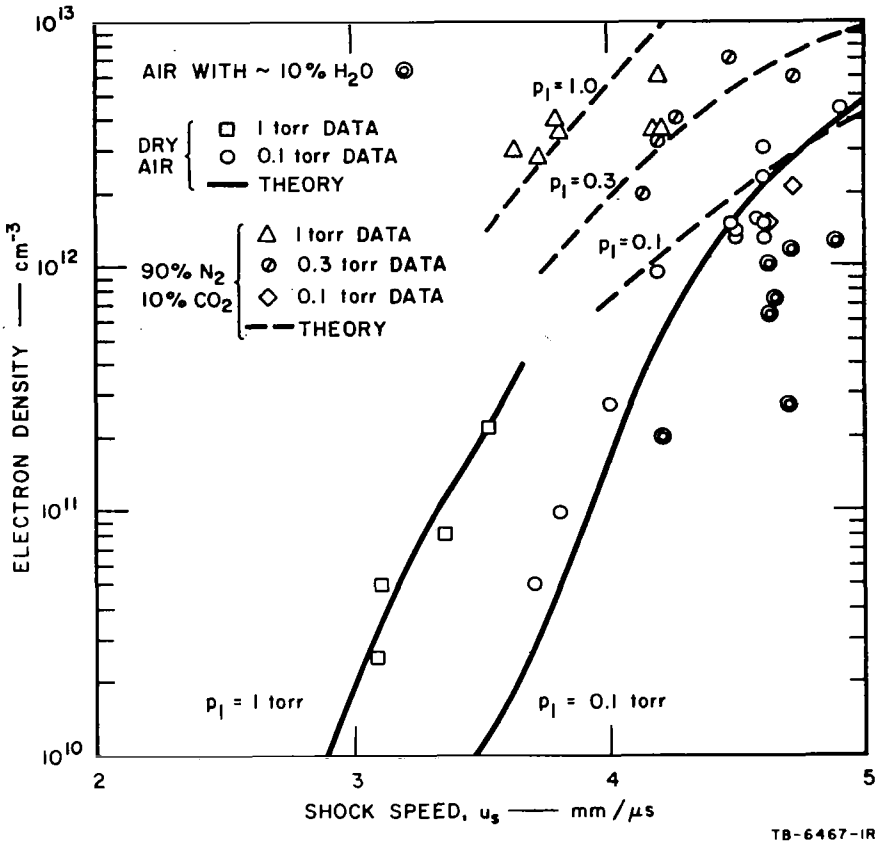

FIG. 18 EQUILIBRIUM ELECTRON DENSITY AS A FUNCTION OF SHOCK SPEED FOR VARIOUS GASES AND PRESSURES

B. N_2/CO_2 Mixtures

Tests were made in various mixtures of N_2 and CO_2 following the series in air, since, according to best authority, these gases comprise the atmospheres of Venus and Mars. Most of these were made in 90 percent N_2/10 percent CO_2. The data from this mixture were found to vary systematically over a wide range of $p_1\tau$ similar to the air data, as shown in Fig. 19. It is seen that the rise times are longer (slower) than in air over the range of shock speed tested. The measurements at p_1 = 0.3 and 1.0 torr were made with three wedge probes mounted 3 inches apart on a line transverse to the tube axis (see Fig. 20). The measurements at p_1 = 0.1 torr were made with six wire probes mounted in

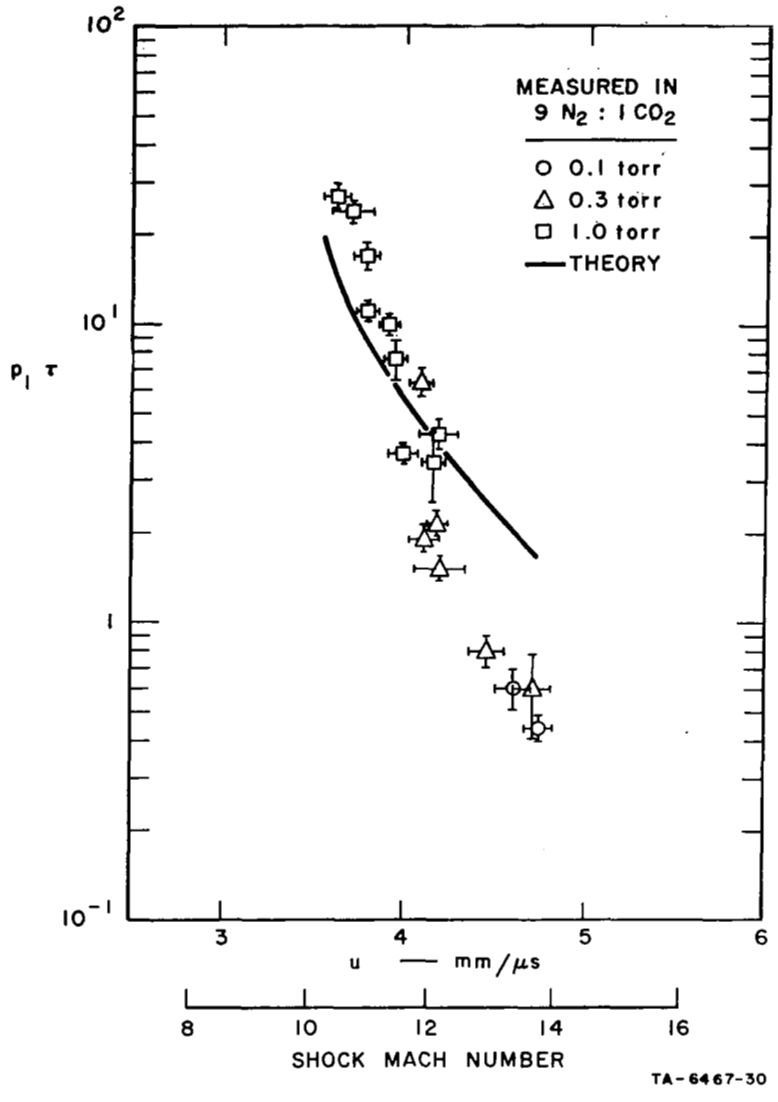

FIG. 19 NORMALIZED IONIZATION RISE TIME MEASURED AND PREDICTED IN 9 N_2:1CO_2 MIXTURES, VERSUS SHOCK SPEED

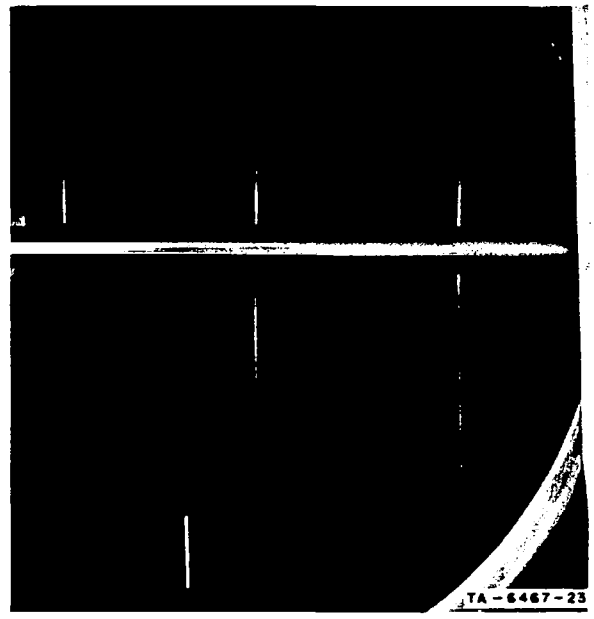

FIG. 20 WEDGE PROBES FOR RISE-TIME MEASUREMENTS

a similar fashion. The spread in the measured times among the various probes determined the vertical error flags of Fig. 19, and the uncertainty in local shock speed, indicated by the horizontal error flags, was determined from spread in the values inferred from the responses of the flush probes placed at regular intervals along the tube (see Fig. 3). The theoretical calculations were made by Evans,[17] using nominal rate constants except for adjustments required to be consistent with Thompson's air calculation.[13]

Figures 21 and 22 are examples of the measured ionization density increase behind the front in this mixture. It can be seen, especially in the lower trace of Fig. 21, that disturbances in the nominal test slug occur in this mixture ahead of the driver-gas interface. The departure from the maximum early slope, seen in Figs. 21 and 22 at values less than half equilibrium, is a characteristic predicted[4] for this mixture, as shown in Fig. 23, in sharp contrast to the ramp-like increase in air. Figure 18 shows good agreement of the measurements of n_{eq} with the predictions for this mixture.

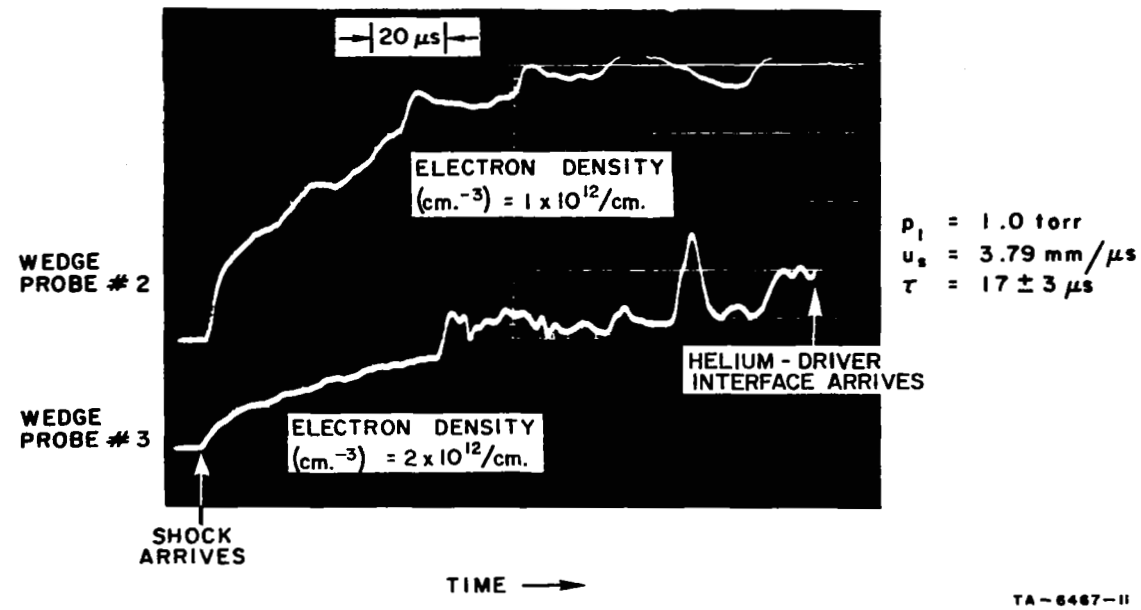

FIG. 21 OSCILLOGRAM OF PROBE CURRENT (two probes, dual traces) AS FUNCTION OF TIME IN 9 N_2:1 CO_2 MIXTURE

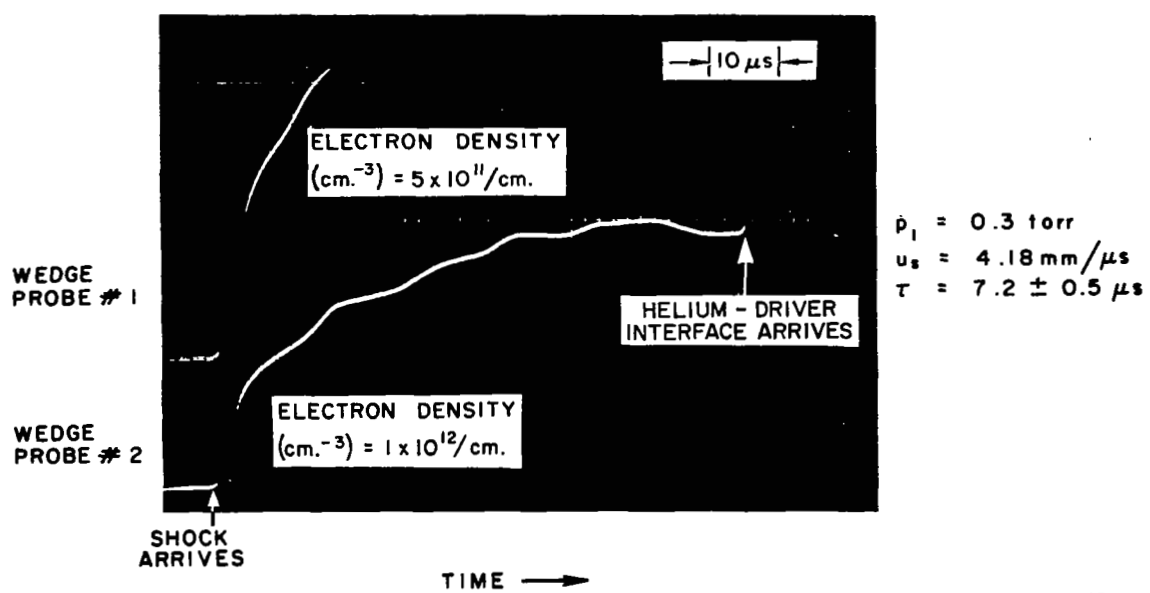

FIG. 22 OSCILLOGRAM OF PROBE CURRENT AS FUNCTION OF TIME IN 9 N_2:1 CO_2 MIXTURE

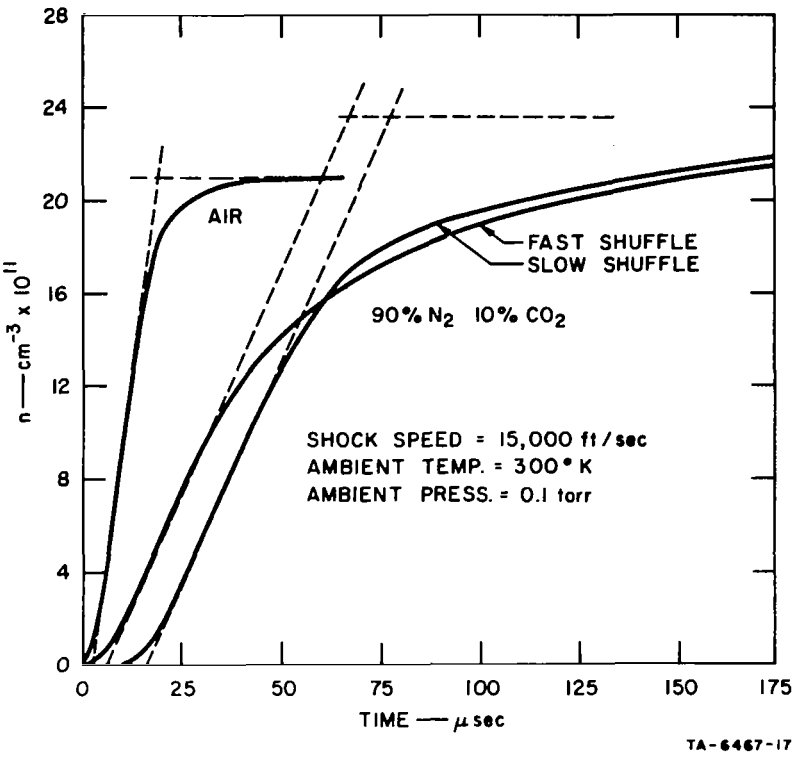

FIG. 23 PREDICTED IONIZATION HISTORY IN AIR AND IN 9 N_2:1 CO_2 MIXTURE

Preliminary measurements in mixtures richer in CO_2 show that the rise times are faster (shorter) and n_{eq} decreases as the CO_2 is increased above 10 percent. However, there was not sufficient data of this kind to construct a universal $p_1\tau$ curve as a function of u_s.

V CONCLUSIONS AND RECOMMENDATIONS FOR FUTURE WORK

The Teflon-plugged slot-admittance measurements showed best agreement with theory when the data are taken in slowly varying plasmas. Parametric calculations from theory show that fine details of the boundary layer profiles are important, such that inaccuracy in determining these layer shapes may be responsible for some of the disagreement with theory.

The ionization rise-time measurements in air served two purposes:

(1) They helped confirm validity of facility and instruments for measuring rise times by virtue of agreement with Frohn and deBoer and with Lin, Neal and Fyfe, at the extremes of the Mach-number range studied

(2) They supplied missing data in the intermediate Mach-number range in good agreement with the calculations of Thompson.

The data in the 90-percent N_2/10-percent CO_2 mixture agree with predictions regarding both equilibrium density and the characteristic "rounded knee" approach to equilibrium, but the measured rise times do not agree satisfactorily with predictions. Preliminary measurements show that rise time is faster as CO_2 percentage is increased from 10 to 50.

Because the ionization history in these complicated gas systems is integrated over many reactions, its measurement can serve as a comparison for predictions, but it is doubtful that it can serve as input data for predictions. It is recommended that similar measurements be undertaken in simpler components of these mixtures in order that better determination of basic reaction rates can be made.

On the other hand, it may be found that a parametric computational study can be made to find a unique set of rates that predict the rise times observed in various mixtures. In this case, measurements in the CO_2-rich mixtures should be resumed.

REFERENCES

1. W. C. Taylor, "The Effects of a Plasma in the Near-Zone Field of an Antenna," Final Report, Contract NAS1-3099, SRI Project 4555, Stanford Research Institute, Menlo Park, California (June 1964).

2. W. C. Taylor, "Study of the Effects of a Plasma in the Near-Zone Field on an Antenna," NASA CR-611 (1966).

3. C. T. Swift, "The Input Admittance of a Rectangular Aperture Covered with Inhomogeneous, Lossy Dielectric Slab," NASA TND-4197, Langley Research Center, Hampton, Virginia (September 1967).

4. C. T. Swift, W. F. Croswell, and J. S. Evans, "Diagnosis of Planetary Atmospheres from Effects of Entry Plasma on Antenna Impedance," Presented at the Sixth Aerospace Sciences Meeting of AIAA, New York, New York (22-24 January 1968).

5. J. C. Camm and P. H. Rose, "Electric Arc-Driven Shock Tube," Phys. Fluids, Vol. 6, No. 5, pp. 663-678 (May 1963).

6. H. R. Bredfeldt, W. E. Scharfman, H. Guthart, and T. Morita, "The Use of Ion Probes in Re-Entry Physics," Tech. Report 26, Contract SD-103 under ARPA Order 281-62, SRI Project 3857, Stanford Research Institute, Menlo Park, California (May 1965).

7. J. G. Kelley, M. A. Levine, A. L. Besse, and A. Tartarian, "Improved Driver Chamber for Arc-Driven Shock Tube," Rev. Sci. Instru., Vol. 38, No. 5, pp. 641-645 (May 1967).

8. W. E. Scharfman, "The Use of Langmuir Probes to Determine the Electron Density Surrounding Re-Entry Vehicles," Final Report, Contract NAS1-2967, SRI Project 4556, Stanford Research Institute, Menlo Park, California (January 1964).

9. W. E. Scharfman, "The Use of Langmuir Probes to Determine the Electron Density Surrounding Re-Entry Vehicles," Final Report, Contract NAS1-3942, SRI Project 5034, Stanford Research Institute, Menlo Park, California (June 1965).

10. W. E. Scharfman and H. R. Bredfeldt, "Use of the Langmuir Probe to Determine the Electron Density and Temperature Surrounding Re-Entry Vehicles," Final Report, Contract NAS1-4872, SRI Project 5771, Stanford Research Institute, Menlo Park, California (December 1966).

11. E. L. Ginzton, Microwave Measurements, Chapter 5 (McGraw-Hill Book Co., Inc., New York, New York, 1957).

12. W. F. Croswell, W. C. Taylor, C. T. Swift, and C. R. Cockrell, "The Input Admittance of a Rectangular Waveguide Fed Aperture Under an Inhomogeneous Plasma: Theory and Experiment," (to be published IEEE Trans. Ant. and Prop., July 1968).

13. W. P. Thompson, "Ionization and NO Production in Air at 3000°-5000°K," Bull. Am. Phys. Soc., Vol. 10, p. 727 (1965).

14. A. Frohn and P. C. T. deBoer, "Ion Density Profiles Behind Shock Waves in Air," AIAA Fifth Aerospace Sciences Meeting, Paper No. 67-94, New York, New York (January 1967).

15. S. C. Lin, R. A. Neal, and W. I. Fyfe, "Rate of Ionization Behind Shock Waves in Air II: Theoretical Interpretations," Phys. Fluids, Vol. 6, pp. 355-375 (1963).

16. P. C. T. deBoer, "Probe for Measuring Ion Density in Slightly Ionized, High-Speed Flow," Rev. Sci. Instr., Vol. 37, pp. 775-785 (1966).

17. J. S. Evans, Private Communication.

NATIONAL AERONAUTICS AND SPACE ADMINISTRATION
WASHINGTON, D.C. 20546

OFFICIAL BUSINESS

FIRST CLASS MAIL

POSTAGE AND FEES PAID
NATIONAL AERONAUTICS AND
SPACE ADMINISTRATION

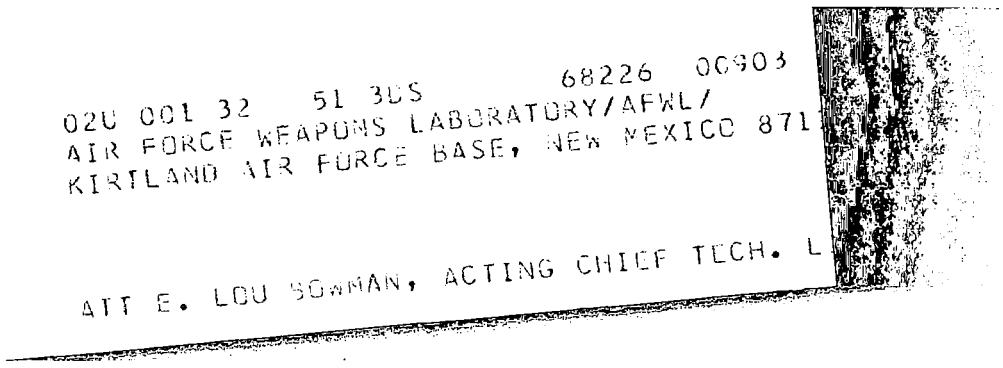

POSTMASTER: If Undeliverable (Section 158 Postal Manual) Do Not Return

"The aeronautical and space activities of the United States shall be conducted so as to contribute . . . to the expansion of human knowledge of phenomena in the atmosphere and space. The Administration shall provide for the widest practicable and appropriate dissemination of information concerning its activities and the results thereof."

—NATIONAL AERONAUTICS AND SPACE ACT OF 1958

NASA SCIENTIFIC AND TECHNICAL PUBLICATIONS

TECHNICAL REPORTS: Scientific and technical information considered important, complete, and a lasting contribution to existing knowledge.

TECHNICAL NOTES: Information less broad in scope but nevertheless of importance as a contribution to existing knowledge.

TECHNICAL MEMORANDUMS: Information receiving limited distribution because of preliminary data, security classification, or other reasons.

CONTRACTOR REPORTS: Scientific and technical information generated under a NASA contract or grant and considered an important contribution to existing knowledge.

TECHNICAL TRANSLATIONS: Information published in a foreign language considered to merit NASA distribution in English.

SPECIAL PUBLICATIONS: Information derived from or of value to NASA activities. Publications include conference proceedings, monographs, data compilations, handbooks, sourcebooks, and special bibliographies.

TECHNOLOGY UTILIZATION PUBLICATIONS: Information on technology used by NASA that may be of particular interest in commercial and other non-aerospace applications. Publications include Tech Briefs, Technology Utilization Reports and Notes, and Technology Surveys.

Details on the availability of these publications may be obtained from:

SCIENTIFIC AND TECHNICAL INFORMATION DIVISION

NATIONAL AERONAUTICS AND SPACE ADMINISTRATION

Washington, D.C. 20546